



HAL
open science

Asymptotic Expansion of a Multiscale Numerical Scheme for Compressible Viscous Multiphase Flows

Remi Abgrall, Maria Giovanna Rodio

► **To cite this version:**

Remi Abgrall, Maria Giovanna Rodio. Asymptotic Expansion of a Multiscale Numerical Scheme for Compressible Viscous Multiphase Flows. [Research Report] RR-7920, INRIA. 2012. hal-00684265

HAL Id: hal-00684265

<https://inria.hal.science/hal-00684265>

Submitted on 31 Mar 2012

HAL is a multi-disciplinary open access archive for the deposit and dissemination of scientific research documents, whether they are published or not. The documents may come from teaching and research institutions in France or abroad, or from public or private research centers.

L'archive ouverte pluridisciplinaire **HAL**, est destinée au dépôt et à la diffusion de documents scientifiques de niveau recherche, publiés ou non, émanant des établissements d'enseignement et de recherche français ou étrangers, des laboratoires publics ou privés.



Asymptotic Expansion of a Multiscale Numerical Scheme for Compressible Viscous Multiphase Flows

Rémi Abgrall, Maria Giovanna Rodio

**RESEARCH
REPORT**

N° 7920

March 30, 2012

Project-Team Bacchus



Asymptotic Expansion of a Multiscale Numerical Scheme for Compressible Viscous Multiphase Flows

Rémi Abgrall, Maria Giovanna Rodio

Project-Team Bacchus

Research Report n° 7920 — March 30, 2012 — 29 pages

Abstract: An asymptotic development of a numerical scheme for the simulation of compressible multiphase flows including viscous effects is illustrated. First, a numerical approximation of the Navier-Stokes equations for each phase is provided. Then, an average procedure of this approximation is used to define, in a probabilistic framework, all the interactions between the two phases. This enables an accurate resolution method for all terms. Thus, the proposed scheme is used for the discretization of a seven-equations model, including relaxation terms that allow obtaining the pressure and velocity equilibrium between the two phases. Finally, an asymptotic analysis at the discrete level is performed, where the relaxation terms disappear. The influence of the viscous terms is studied, comparing the results obtained by solving the Navier-Stokes equations (validated with reference solutions given in the literature) with the Euler solutions.

Key-words: Two-phase flows, Pressure and velocity equilibrium, Viscous flows, Compressible interface problems

**RESEARCH CENTRE
BORDEAUX – SUD-OUEST**

351, Cours de la Libération
Bâtiment A 29
33405 Talence Cedex

Développement asymptotique d'un schéma numérique pour un écoulement compressible, visqueux et diphasique

Résumé : Le développement asymptotique d'un schéma pour la simulation d'un écoulement diphasique compressibles avec des effets visqueux est illustré. Tout d'abord, une approximation numérique des équations de Navier-Stokes pour chaque phase est développée. Ensuite, une procédure de moyenne de cette approximation est appliquée pour définir, dans un cadre probabiliste, toutes les interactions entre les deux phases. Cela permet de fournir une méthode de résolution exacte pour tous les termes. Donc, le schéma discrétise un modèle à sept équations, incluant des termes de relaxation qui permettent d'obtenir l'équilibre de pression et de vitesse entre les deux phases. Enfin, une analyse asymptotique à un niveau discret est présentée, où les termes de relaxation disparaissent. L'influence du terme de viscosité est étudiée, en comparant les résultats obtenus en résolvant les équations de Navier-Stokes (validés avec des solutions de référence donnée dans la littérature) avec les solutions d'Euler.

Mots-clés : Écoulements diphasiques compressibles, Équilibre de pression et de vitesse, Fluides visqueux, Problèmes d'interfaces entre fluides compressibles

Contents

1	Introduction	4
2	The seven-equation model	5
2.1	1D formulation	7
3	Numerical scheme for the seven equations model	8
3.1	Averaging procedure	11
3.2	Second-Order accuracy	14
4	Asymptotic analysis of the numerical scheme	16
4.1	Scheme for the reduced model including viscous effect	17
5	Thermodynamic Closure	20
6	Results	20
6.1	Validation	20
6.1.1	One fluid test-case with very high viscosity	20
6.1.2	Two-fluids test-case with very high viscosities	21
6.1.3	Surana [1] viscous test-case with air	22
6.2	Shock-tube with water	24
6.3	Two-phases flow problem	25
7	Conclusions	25

1 Introduction

Compressible multiphase flows occur in a wide variety of engineering systems. Their numerical simulation is still an open problem from both theoretical and mathematical point of view, due to complexities of describing the interactions between two phases separated by an interface.

In literature, several numerical methods exist [2, 3, 4, 5, 6]. In particular, the so-called discrete equation method (DEM), initially proposed by Abgrall and Saurel [7] (see also [8]) results in a well-posed hyperbolic system and it presents some properties able to handle non-conservative terms and to solve interface problems without conservation errors. In particular, the originality of DEM is based on the probabilistic approach in order to avoid the questionable determination of average variables.

Initially, the DEM was proposed for compressible multiphase flows basing on seven equations system (three conservative equations for each phase and a transport equation for the volume fraction). This corresponds to the case of two compressible phases. In this model, some relaxation terms appear in order to drive the system toward pressure and velocity equilibrium.

However, as remarked by Murrone et al. [9], these methods are more complex from a numerical point of view and they present a sensitivity of the results with respect to the relaxation procedures for the pressure and the velocity. Thus, more recent works [9, 10] proposed an homogeneous Eulerian model for the simulation of compressible two-phase flow problems based on a five equations system (the conservative equations of momentum and energy are calculated for the mixture). Abgrall and Perrier [11] proposed an asymptotic expansion starting from the discrete scheme for an Eulerian formulation.

The validity of DEM has been amply demonstrated, reproducing unsteady wave propagation in inviscid flow, even if viscous effects have been occasionally taken into account [10]. However, viscous effects is of primary importance for a predictive simulation of multiphase flows, where the viscosity play a major role in the complex interaction between the interface and the compression shocks.

In this work, we focus on the analysis of viscous effects influence in the simulation of dispersed two-phase flows. More precisely, a semi discrete scheme is proposed in order to model a reduced equations system where viscous effects are taken into account.

This analysis follows the work illustrated in [11, 9], *i.e.* an asymptotic expansion has been developed in which the relaxation terms linked to interface convective fluxes disappear, obtaining in this way the reduced discrete scheme. We develop a numerical approximation of compressible viscous multiphase flows relying on Godunov scheme and relaxation solver.

The work is organized as follows. In section 2, we give a description of the seven equation model with viscous effects. In section 3, we derive a semi-discrete numerical approximation of the two-phase model. Then, we performed an average procedure of the discrete approximation and an extension to the second-order. In section 4, we analyse the asymptotic expansion in order to obtain a semi-discrete approximation for a reduced five-equation model. In section 6, several test-cases are considered for the assessment of the proposed formulation.

2 The seven-equation model

Let us start by illustrating the seven-equations model taking into account viscous effects. For each phase k , the single-phase Navier-Stokes equations can be written in the following form:

$$\frac{\partial}{\partial t} \begin{pmatrix} \rho^k \\ \rho^k \vec{v}^k \\ \rho^k E^k \end{pmatrix} + \nabla \cdot \begin{pmatrix} \rho^k \vec{v}^k \\ \rho^k \vec{v}^k \otimes \vec{v}^k + P^k \bar{\bar{\mathbb{I}}} - \bar{\bar{\tau}}^k \\ \rho u^k E^k + P^k \bar{\bar{\mathbb{I}}} - \bar{\bar{\tau}}^k \cdot \vec{v}^k \end{pmatrix} = \begin{pmatrix} \dot{m} \\ \dot{m} \vec{v}^k + f_d^k \\ \dot{m} E^k + f_d \vec{v}^k + Q \end{pmatrix} \quad (1)$$

i.e.

$$\frac{\partial U^k}{\partial t} + \bar{\nabla} \cdot (\bar{F}^k - \bar{F}_v^k) = S, \quad (2)$$

in which ρ_k , α_k , \vec{v}^k , P_k and τ_k are the fluid density, the volume fraction, the velocity vector, the pressure and the stress tensor for each phase $k = 1, 2$ respectively. The total energy, E_k is defined as:

$$E^k = \bar{\varepsilon}^k + \frac{1}{2} \bar{u}_k \cdot \bar{u}_k.$$

U is the vector of conservative variables and the right-hand side is represented by the source vector S . The flux vector presents two components, the inviscid flux \bar{F} and the viscous contribution \bar{F}_v .

We assume a Newtonian fluid defined by two viscosity coefficients λ and μ . The shear stress tensor $\bar{\tau}$ becomes:

$$\bar{\tau}_{ij} = \mu(\partial_i v_j + \partial_j v_i) + \lambda(\bar{\nabla} \cdot \vec{v}) \delta_{ij} \quad \text{with } i, j = x, y, z$$

We consider that the Stokes relation $3\lambda + 2\mu = 0$ is valid. Hence the shear stresses is re-written as:

$$\bar{\tau}_{ij} = \mu(\partial_i v_j + \partial_j v_i) - \frac{2}{3} \mu(\bar{\nabla} \cdot \vec{v}) \delta_{ij} \quad (3)$$

Now we introduce, as in [12], the characteristic function X^k of the phase Σ_k : $X^k(x, t) = 1$ if x lies in the fluid Σ_k at time t and 0 otherwise. The function X^k satisfies the topological equation

$$\frac{\partial X^k}{\partial t} + \sigma \cdot \nabla X^k = 0, \quad (4)$$

where σ is the interface velocity between the two phases.

An averaging procedure similar to that used by Drew [12] is applied to system 1. Remark that energy term source, Q , is neglected.

As explained in Saurel and Abgrall [5], after propagation of the shock waves, the gas/liquid system evolves after a more or less long time period to an equilibrium state that will tend to $P_{gas} \approx P_{liquid}$. The waves propagation creates a volume variation of each fluid, accompanied by an internal energy variation, so the pressure relaxation undergoes a volume variation given by the equation:

$$\frac{\partial \alpha_g}{\partial t} = \mu_r (P_g - P_l) \quad \text{with } l = \text{liquid } v = \text{vapor} \quad (5)$$

and the volume variation induces the energy variations due to the interfacial pressure work

$$\frac{\partial \alpha_k \rho_k E_k}{\partial t} = -\mu_r P_I (P_g - P_l), \quad (6)$$

where μ represents the dynamic compaction viscosity (it is different by fluid dynamic viscosity). The velocities also relax to an equilibrium state, but with a characteristic time that is longer than for the pressure. Thus, the velocity relaxation is represented by drag force f_d term that becomes:

$$f_d = \lambda(u_l - u_g), \quad (7)$$

where λ is a parameter (given later). μ_r and λ depend on the interfacial area.

With the introduction of Eq.(4) - Eq.(7), the averaged system(1) can be written as

$$\left\{ \begin{array}{l} \frac{\partial \bar{\alpha}^k}{\partial t} = -\mathcal{E}(\sigma \cdot \nabla \bar{\alpha}^k) + \mu_r (P^k - P^{k*}) \\ \frac{\partial \bar{\alpha}^k \bar{\rho}^k}{\partial t} + \nabla(\bar{\alpha}^k \bar{\rho}^k \bar{v}^k) = \mathcal{E}(\rho_I (\bar{v}_I^k - \sigma) \cdot \nabla X^k) \\ \frac{\partial \bar{\alpha}^k \bar{\rho}^k \bar{v}^k}{\partial t} + \nabla(\bar{\alpha}^k \bar{\rho}^k \bar{v}^k \otimes \bar{v}^k + \bar{\alpha}^k \bar{P}^k \mathbb{I}) = \mathcal{E} \left((\rho_I^k \bar{v}_I^k (\bar{v}_I^k - \sigma) + P_I \mathbb{I}) \cdot \nabla X^k \right) + \\ \quad + \nabla \cdot (\bar{\alpha}^k \bar{\tau}^k) - \mathcal{E}(\tau_I \cdot \nabla X^k) + \lambda (\bar{v}^{k*} - \bar{v}^k) \\ \frac{\partial \bar{\alpha}^k \bar{\rho}^k \bar{E}^k}{\partial t} + \nabla(\bar{\alpha}^k (\bar{\rho}^k \bar{E}^k \bar{v}^k + \bar{P}^k \mathbb{I} \bar{v}^k)) = \mathcal{E} \left((\rho_I E_I (\bar{v}_I^k - \sigma) + P_I \mathbb{I}) \cdot \nabla X^k \right) + \\ \quad + \lambda \bar{v}_I^k (\bar{v}^{k*} - \bar{v}^k) + \mu_r P_I (P^k - P^{k*}) \\ \quad + \nabla \cdot (\bar{\alpha}^k (\bar{\tau}^k \cdot \bar{v}_I^k)) - \mathcal{E}((\tau_I \bar{v}^k) \cdot \nabla X^k) \end{array} \right. \quad (8)$$

where P^{k*} and \bar{v}^{k*} are the variables of the other phase. More attention should be given on the right terms in which a difference of velocity ($u_I - \sigma$) appears. These terms represent the mass transfer, \dot{m} , between the two phases and in the case in which mass transfer is neglected, the two velocities are equal. In this work, no mass transfer is considered, *i.e.* $u_I = \sigma$.

Thus, the system (8), that is coupled to closing equations, is capable to model non-equilibrium two-phase mixtures in presence of viscous effects.

In the limit of $\lambda, \mu \rightarrow +\infty$, the asymptotic expansion of model (8) has been obtained by Perigaud and Saurel [10], using some known relations [5, 12] for which $\mathcal{E}(P^k \nabla X^k) = P_I \nabla \alpha^k$, $\mathcal{E}((P^k \bar{v}) \nabla X^k) = P_I u_I \nabla \alpha^k$ and $\mathcal{E}(\sigma \nabla X^k) = u_I \nabla \alpha^k$:

$$\left\{ \begin{array}{l} \frac{\partial \bar{\alpha}^1}{\partial t} = -\bar{v} \cdot \nabla \alpha^1 + K \nabla(\bar{v}) \\ \frac{\partial \alpha^1 \rho^1}{\partial t} + \nabla(\alpha^1 \rho^1 \bar{v}) = 0 \\ \frac{\partial \alpha^2 \rho^2}{\partial t} + \nabla(\alpha^2 \rho^2 \bar{v}) = 0 \\ \frac{\partial \rho \bar{v}}{\partial t} + \nabla(\rho^k \bar{v} \otimes \bar{v} + P) = \nabla \tau \\ \frac{\partial E}{\partial t} + \nabla(E + P) = \nabla \tau \cdot \bar{v} \end{array} \right. \quad (9)$$

where ρ is the mixture density, defined as $\rho = \alpha_1 \rho_1 + \alpha_2 \rho_2$ and $K = \alpha_1 \alpha_2 (\rho_2 c_2^2 - \rho_1 c_1^2) / (\alpha_1 \rho_2 c_2^2 + \alpha_2 \rho_1 c_1^2)$.

2.1 1D formulation

When a one-dimension (1D) flow is considered, it is possible to operate several simplification. In x Cartesian coordinates, the components of viscous flux \vec{F}_v becomes [13]:

$$\begin{aligned}\tau_{xx} &= 2\mu \frac{\partial u}{\partial x} - \frac{2}{3}\mu(\nabla \cdot \vec{v}) = \frac{4}{3}\mu \frac{\partial u}{\partial x} \\ \tau_{xx}u &= 2\mu u \frac{\partial u}{\partial x} - \frac{2}{3}\mu(\nabla \cdot \vec{v})u = \frac{4}{3}\mu \frac{\partial u}{\partial x} u\end{aligned}\quad (10)$$

Moreover, into the system (8) a viscous flux at the interface comes out. This term is defined as follows :

$$\begin{aligned}\tau_{Ixx} &= 2\mu \frac{\partial u_I}{\partial x} - \frac{2}{3}\mu(\nabla \cdot \vec{v}_I) = \frac{4}{3}\mu \frac{\partial u_I}{\partial x} \\ \tau_{Ixx}u_I &= 2\mu u_I \frac{\partial u_I}{\partial x} - \frac{2}{3}\mu(\nabla \cdot \vec{v}_I)u_I = \frac{4}{3}\mu \frac{\partial u_I}{\partial x} u_I\end{aligned}\quad (11)$$

Remember that in this work, no mass transfer is considered, the system 8 becomes:

$$\left\{ \begin{array}{l} \frac{\partial \bar{\alpha}^k}{\partial t} = -\mathcal{E} \left(\sigma \frac{\partial X^k}{\partial x}, \right) + \mu_r (P^k - P^{k*}) \\ \frac{\partial \bar{\alpha}^k \bar{\rho}^k}{\partial t} + \frac{\partial (\bar{\alpha}^k \bar{\rho}^k \bar{u}^k)}{\partial x} = 0 \\ \frac{\partial \bar{\alpha}^k \bar{\rho}^k \bar{u}^k}{\partial t} + \frac{\partial}{\partial x} (\alpha^k \rho^k (u^k)^2 + \alpha^k P^k) = \mathcal{E} \left(P_I \frac{\partial X^k}{\partial x} \right) + \lambda (u^{k*} - u^k) + \\ \quad + \frac{\partial}{\partial x} \left(\bar{\alpha}^k \frac{4}{3} \mu \frac{\partial u}{\partial x} \right) - \mathcal{E} \left(\frac{4}{3} \mu \frac{\partial u_I}{\partial x} \frac{\partial X^k}{\partial x} \right) \\ \frac{\partial \bar{\alpha}^k \bar{\rho}^k \bar{E}^k}{\partial t} + \frac{\partial}{\partial x} (\alpha^k \rho^k \bar{E}^k \bar{u}^k + \bar{P}^k \mathbb{1} \bar{u}^k) = \mathcal{E} \left(P_I \frac{\partial X^k}{\partial x} \right) + \lambda u_I^k (\bar{u}^{k*} - \bar{u}^k) + \mu_r P_I (P^k - P^{k*}) \\ \quad + \frac{\partial}{\partial x} \left(\bar{\alpha}^k \frac{4}{3} \mu \frac{\partial u^k}{\partial x} u^k \right) + \mathcal{E} \left(\frac{4}{3} \mu \frac{\partial u_I}{\partial x} u_I \frac{\partial X^k}{\partial x} \right) \end{array} \right. \quad (12)$$

where P_I and v_I are the values of pressure, velocity and stresses at the interface on the component k of the interface. In the literature, several expression are given. In previous works [7, 14], a sophisticated estimation have been proposed:

$$\left\{ \begin{array}{l} P_I^k = \frac{Z^k P^{k*} + Z^{k*} P^k}{Z^k + Z^{k*}} + \text{sign} \left(\frac{\partial \alpha^k}{\partial x}, \right) \frac{(u^{k*} - u^k)}{Z^k + Z^{k*}} \\ v_I^k = \frac{Z^k u^k + Z^{k*} u^{k*}}{Z^k + Z^{k*}} + \text{sign} \left(\frac{\partial \alpha^k}{\partial x}, \right) \frac{P^{k*} + P^k}{Z^k + Z^{k*}} \end{array} \right. \quad (13)$$

where Z^k represents the acoustic impedance, *i.e.* $Z = \rho c$, where c is the speed of sound.

Remark the difference between the μ and μ_r , where the first one is the fluid dynamic viscosity, defined as $\mu = \alpha \mu_1 + (1 - \alpha) \mu_2$, while the second one is a relaxation parameter. Along with the other relaxation parameter λ , it has been defined as:

$$\mu_r = \frac{S_I}{Z_1 + Z_2}, \quad \lambda = Z_1 Z_2 \mu_r$$

where S_I is the exchange surface. In the present contribution, our purposes are (i) to derive a semi-discrete numerical approximation of the system (11)

following the technique of Abgrall and Saurel [7] and then (ii) to develop an asymptotic expansion from discrete scheme as in Abgrall and Perrier [11], considering also the viscous fluxes and thus, to obtain the semi-discrete numerical approximation of the system (9) in one-dimensional form.

3 Numerical scheme for the seven equations model

Here, our purpose is to obtain a semi-discrete numerical approximation of the two-phase system including the viscous term (Eq. 8), following the same procedure of [7].

We describe this scheme for a finite volume type in the case of a Godunov solver, but the procedure can be adapted to other solvers. Let us define our space-time domain on which we can compute the solution. At time t , the computational domain Ω is divided into a *constant* number of volume control $\mathcal{C}_i =]x_{i-1/2}, x_{i+1/2}[$. In addition, each volume control \mathcal{C}_i is divided into a random subdivision $x_{i-1/2} = \xi_0 < \xi_1 < \dots < \xi_{N(\omega)} = x_{i+1/2}$ (where ω is a random parameter).

In each subcell $]\xi_l, \xi_{l+1}[$, X^k is constant and so only one phase Σ_k can exist. Neglecting the source terms S of Eq.2, the integral form of Navier-Stokes equations for the space-time domain $\mathcal{C}_i \times [t, t + s]$ is

$$\int_t^{t+s} \int_{\mathcal{C}_i} X \frac{\partial U}{\partial t} + \int_t^{t+s} \int_{\mathcal{C}_i} X \frac{\partial(F - F_v)}{\partial x} dx dt = 0 \quad (14)$$

The Godunov scheme is no longer applied on the mesh cells, but on the modified and non-uniform cells constructed according to the position of the interface.

$\sigma_{i+1/2} = \sigma(U_i, U_{i+1})$ denotes the speeds of interface between the two cells \mathcal{C}_i and \mathcal{C}_{i+1} . It will be clearly equal to zero, if into the cells there is the same phase, otherwise $\sigma_{i+1/2}$ coincides with the speed of propagation of the interface in the Riemann solution $(x, t) \rightarrow v_r(\frac{x}{t}; U_i, U_{i+1})$.

Thus, assuming that between the times t^n and $t^{n+1} = (t + s)$, the interface $x_{i+1/2}$ moves at velocity $\sigma_{i+1/2}$, the cell \mathcal{C}_i is not fixed, but it evolves in $\tilde{\mathcal{C}}_i =](x_{i-1/2} + s\sigma_{i-1/2}), (x_{i+1/2} + s\sigma_{i+1/2})[$ (see Fig.1). The cell may be either smaller or larger than the original ones \mathcal{C}_i , depending on the signs of the velocities $\sigma_{i+1/2}$.

We denote $F(U_L, U_R)$ the Godunov numerical flux between the states U_L and U_R and $F^{lag}(U_L, U_R)$ the flux across the contact discontinuity between the states U_L and U_R (see Fig.2) and we have:

$$F^{lag}(U_L, U_R) = F(U_{LR}^+) - \sigma(U_L, U_R)U_{LR}^+ = F(U_{LR}^-) - \sigma(U_L, U_R)U_{LR}^-$$

Considering Fig.1, the previous integral (Eq.14), defined on the mesh cell \mathcal{C}_i , can be divided into three contributions, *i.e.* the integrals on abb' for the left boundary, the integral on bcc' for the right boundary and the Lagrangian internal cells. Thus Eq.14 can be rewritten as

$$\begin{aligned} & \int_{abb'} X \left[\frac{\partial U}{\partial t} + \frac{\partial(F - F_v)}{\partial x} \right] dx dt + \quad (I) \\ & + \sum_{l=2}^{N(\omega)-2} \int_t^{t+s} \int_{\xi_{l+s\sigma(U_i^{l-1}, U_i^l)}^l}^{\xi_{l+1+s\sigma(U_i^l, U_i^{l+1})}^l} X \left[\frac{\partial U}{\partial t} + \frac{\partial(F - F_v)}{\partial x} \right] dx dt + \quad (II) \end{aligned}$$

$$+ \int_{acc'} X \left[\frac{\partial U}{\partial t} + \frac{\partial(F - F_v)}{\partial x} \right] dx dt = 0 \quad (III)$$

Including the characteristic function X in derivative terms and applying the Godunov scheme, we obtain for each term, the solution at time $t + s$. For the boundary terms (I) and (III), it is important to remark that the domain where computing the integral is a triangle. At time t we have only one point (a) and thus the spatial integral is zero.

Remembering that the characteristic function obeys to the following property:

$$\sum_{l=0}^{N(\varpi)-1} \int_t^{t+s} \int_{\xi_l}^{\xi_{l+1}} \frac{\partial X}{\partial t} dx dt + \sum_{l=0}^{N(\varpi)-1} \int_t^{t+s} \int_{\xi_l}^{\xi_{l+1}} \sigma \frac{\partial X}{\partial x} dx dt = 0, \quad (16)$$

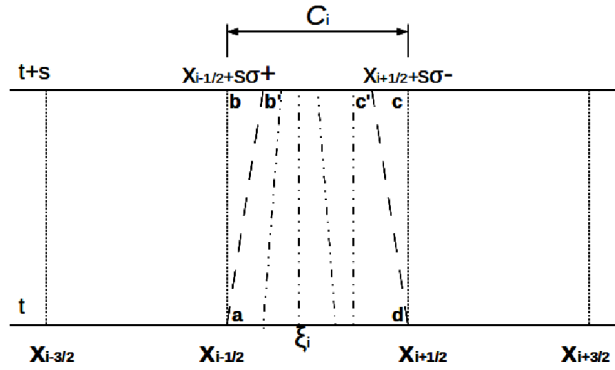


Figure 1: Subdivision of computational domain.

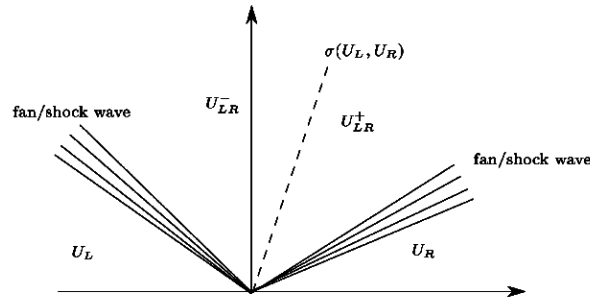


Figure 2: The various states in the Riemann problem between states U_L and U_R .

we can write for (I)

$$\begin{aligned}
& \int_{abb'} X \left[\frac{\partial U}{\partial t} + \frac{\partial(F - F_v)}{\partial x} \right] dx dt = \\
& \int_{abb'} \left[\frac{\partial XU}{\partial t} + \frac{\partial X(F - F_v)}{\partial x} \right] dx dt - \int_{abb'} \left[U \frac{\partial X}{\partial t} + (F - F_v) \frac{\partial X}{\partial x} \right] dx dt = \\
& \int_{x_{i-1/2}}^{x_{i-1/2} + s\sigma^+(U_{i-1}^+, U_i^-)} X(x, t+s)U(x, t+s) dx - sX(x_{i-1/2}, t)F(U_{i-1/2}^*) + \\
& -sF^{lag}(U_{i-1}^+, U_i^-)[X]_{j=0} + \mathbf{sX}(\mathbf{x}_{i-1/2}, \mathbf{t})\mathbf{F}_v(\mathbf{U}_{i-1/2}^*) + \mathbf{sF}_{vI}(\mathbf{U}_{i-1}^+, \mathbf{U}_i^-)[\mathbf{X}]_{j=0},
\end{aligned}$$

where $U_{i\pm 1/2}^*$ is the solution of the Riemann problem. In this work, no mass transfer is considered, then when a jump is considered, the viscous contribution is zero because there is not transfer of viscous information. Similarly we have for (III)

$$\begin{aligned}
& \int_{dcc'} X \left[\frac{\partial U}{\partial t} + \frac{\partial(F - F_v)}{\partial x} \right] dx dt = \\
& \int_{dcc'} \left[\frac{\partial XU}{\partial t} + \frac{\partial X(F - F_v)}{\partial x} \right] dx dt - \int_{dcc'} \left[U \frac{\partial X}{\partial t} + (F - F_v) \frac{\partial X}{\partial x} \right] dx dt = \\
& \int_{x_{i+1/2}}^{x_{i+1/2} + s\sigma^-(U_i^+, U_{i+1}^-)} X(x, t+s)U(x, t+s) dx + sX(x_{i+1/2}, t)F(U_{i+1/2}^*) + \\
& +sF^{lag}(U_i^+, U_{i+1}^-)[X]_{j=N(w)} - \mathbf{sX}(\mathbf{x}_{i+1/2}, \mathbf{t})\mathbf{F}_v(\mathbf{U}_{i+1/2}^*) - \mathbf{sF}_{vI}(\mathbf{U}_i^+, \mathbf{U}_{i+1}^-)[\mathbf{X}]_{j=N(w)}.
\end{aligned}$$

For the internal terms (II) the integral becomes

$$\begin{aligned}
& \int_t^{t+s} \int_{\xi_j + s\sigma(U_i^{j-1}, U_i^j)}^{\xi_{j+1} + s\sigma(U_i^j, U_i^{j+1})} X \left[\frac{\partial U}{\partial t} + \frac{\partial(F - F_v)}{\partial x} \right] dx dt = \\
& \int_{\xi_j + s\sigma(U_i^{j-1}, U_i^j)}^{\xi_{j+1} + s\sigma(U_i^j, U_i^{j+1})} X(x, t+s)U(x, t+s) dx - \int_{\xi_j}^{\xi_{j+1}} X(x, t)U(x, t) dx + \\
& -s \left(F^{lag}(U_i^j, U_i^{j+1})[X]_j - F^{lag}(U_i^{j-1}, U_i^j)[X]_{j-1}, \right) + \\
& +s \left(\mathbf{F}_v(\mathbf{U}_i^j, \mathbf{U}_i^{j+1})[\mathbf{X}]_j - \mathbf{F}_v(\mathbf{U}_i^{j-1}, \mathbf{U}_i^j)[\mathbf{X}]_{j-1}, \right).
\end{aligned}$$

Summing up all terms, dividing for s and taking the limit when $s \rightarrow 0$, we

obtain the *semi-discrete* scheme

$$\begin{aligned}
 & \frac{\partial}{\partial t} \left(\frac{1}{\Delta x} \int_{x_{i-1/2}}^{x_{i+1/2}} X(x, t) U(x, t) dx \right) + \\
 & + \frac{1}{\Delta x} (X(x_{i+1/2}, t) F(U_{i+1/2}^*) - X(x_{i-1/2}, t) F(U_{i-1/2}^*)) + \\
 & - \frac{1}{\Delta \mathbf{x}} (\mathbf{X}(\mathbf{x}_{i+1/2}, \mathbf{t}) \mathbf{F}_v(\mathbf{U}_{i+1/2}^*) - \mathbf{X}(\mathbf{x}_{i-1/2}, \mathbf{t}) \mathbf{F}_v(\mathbf{U}_{i-1/2}^*)) = \\
 & = \frac{1}{\Delta x} \sum_{j=1}^{N(w)-1} (F^{lag}(U_i^j, U_i^{j+1})[X]_j - F^{lag}(U_i^{j-1}, U_i^j)[X]_{j-1}) + \\
 & + \frac{1}{\Delta x} (F^{lag}(U_i^-, U_{i-1}^+)[X]_{j=0} - F^{lag}(U_i^+, U_{i+1}^-)[X]_{j=N(w)}) + \\
 & - \sum_{j=1}^{N(w)-1} (\mathbf{F}_v(\mathbf{U}_i^j, \mathbf{U}_i^{j+1})[\mathbf{X}]_j - \mathbf{F}_v(\mathbf{U}_i^{j-1}, \mathbf{U}_i^j)[\mathbf{X}]_{j-1}) + \\
 & - \frac{1}{\Delta \mathbf{x}} (\mathbf{F}_v(\mathbf{U}_i^+, \mathbf{U}_{i+1}^-)[\mathbf{X}]_{j=0} - \mathbf{F}_v(\mathbf{U}_i^-, \mathbf{U}_{i-1}^+)[\mathbf{X}]_{j=N(w)}). \tag{17}
 \end{aligned}$$

We may assume that two adjacent subcell contains different phases, so that

$$\begin{aligned}
 & \sum_{j=1}^{N(w)-1} (F^{lag}(U_i^j, U_i^{j+1})[X]_j - F^{lag}(U_i^{j-1}, U_i^j)[X]_{j-1}) = \\
 & = N(\omega)_{int} (F^{lag}(U_i^2, U_i^1) - F^{lag}(U_i^1, U_i^2)) \tag{18}
 \end{aligned}$$

and

$$\begin{aligned}
 & \sum_{j=1}^{N(w)-1} (\mathbf{F}_v(\mathbf{U}_i^j, \mathbf{U}_i^{j+1})[\mathbf{X}]_j - \mathbf{F}_v(\mathbf{U}_i^{j-1}, \mathbf{U}_i^j)[\mathbf{X}]_{j-1}) = \\
 & = N(\omega)_{int} (F_v(U_i^2, U_i^1) - F_v(U_i^1, U_i^2)) \tag{19}
 \end{aligned}$$

3.1 Averaging procedure

Now, it is possible to apply the averaging procedure as done into the system (8), but to discrete equations system (17), instead of the system of PDE. Taking the mathematical expectancy of the semidiscrete scheme (Eq.17) for which we have:

$$\frac{\partial}{\partial t} \left(\frac{1}{\Delta x} \int_{x_{i-1/2}}^{x_{i+1/2}} X(x, t) U(x, t) dx \right) = \frac{\partial \alpha_i^{(1)} U_i^{(1)}}{\partial t} \tag{20}$$

and introducing the notation for the average number of internal interfaces:

$$\lambda_i = \mathcal{E} \left(\frac{N(\omega)_{int}}{\Delta x} \right),$$

The scheme can be rewritten as:

$$\begin{aligned}
& \frac{\partial \alpha_i^{(1)} U_i^{(1)}}{\partial t} + \frac{1}{\Delta x} \mathcal{E} \left(X(x_{i+1/2}, t) F(U_{i+1/2}^*) - X(x_{i-1/2}, t) F(U_{i-1/2}^*) \right) + \\
& - \frac{1}{\Delta \mathbf{x}} \mathcal{E} \left(\mathbf{X}(\mathbf{x}_{i+1/2}, \mathbf{t}) \mathbf{F}_v(\mathbf{U}_{i+1/2}^*) - \mathbf{X}(\mathbf{x}_{i-1/2}, \mathbf{t}) \mathbf{F}_v(\mathbf{U}_{i-1/2}^*) \right) = \\
& + \frac{1}{\Delta x} \mathcal{E} \left(F^{lag}(U_i^-, U_{i-1}^+) [X]_{j=0} - F^{lag}(U_i^+, U_{i+1}^-) [X]_{j=N(w)} \right) + \\
& - \frac{1}{\Delta \mathbf{x}} \mathcal{E} \left(\mathbf{F}_{v\mathbf{I}}(\mathbf{U}_i^+, \mathbf{U}_{i-1}^-) [\mathbf{X}]_{j=0} - \mathbf{F}_{v\mathbf{I}}(\mathbf{U}_i^-, \mathbf{U}_{i+1}^+) [\mathbf{X}]_{j=N(w)} \right) \\
& + \lambda_i \left(F^{lag}(U_i^2, U_i^1) - F^{lag}(U_i^1, U_i^2) \right) - \lambda_i \left((F_v(U_i^2, U_i^1) - F_v(U_i^1, U_i^2)) \right)
\end{aligned} \tag{21}$$

In [7], the definition of all the terms, both conservative and non-conservative, have been given, except the terms in which viscous flux appears. Let us remember only some necessary definitions already used in [7]. We consider the cell boundary $i + 1/2$ and focus on the fluxes available for fluid Σ_1 . On this cell boundary, four instances may occur on the base of the phase present in the cell x_i and in the cell x_{i+1} (see Tab.1). Thus, we can define the flux indicator

$$\beta_{i+1/2}^{(l,r)} = \text{sign}(\sigma(U_i^l, U_{i+1}^r)) = \begin{cases} 1 & \text{if } \sigma(U_i^l, U_{i+1}^r) \geq 0, \\ -1 & \text{if } \sigma(U_i^l, U_{i+1}^r) < 0 \end{cases}$$

and the corresponding probability to have the same phase or two different phases into the left and right cell of cell boundary $i + 1/2$

$$\begin{aligned}
P_{i+1/2}(\Sigma_1, \Sigma_1) &:= P \left(X(x_{i+1/2}^-) = 1 \text{ and } X(x_{i+1/2}^+) = 1 \right) = \min \left(\alpha_i^{(1)}, \alpha_{i+1}^{(1)} \right) \\
P_{i+1/2}(\Sigma_1, \Sigma_2) &:= P \left(X(x_{i+1/2}^-) = 1 \text{ and } X(x_{i+1/2}^+) = 0 \right) = \max \left(\alpha_i^{(1)} - \alpha_{i+1}^{(1)}, 0 \right) \\
P_{i+1/2}(\Sigma_2, \Sigma_1) &:= P \left(X(x_{i+1/2}^-) = 0 \text{ and } X(x_{i+1/2}^+) = 1 \right) = \max \left(\alpha_i^{(2)} - \alpha_{i+1}^{(2)}, 0 \right) \\
P_{i+1/2}(\Sigma_2, \Sigma_2) &:= P \left(X(x_{i+1/2}^-) = 0 \text{ and } X(x_{i+1/2}^+) = 0 \right) = \min \left(\alpha_i^{(2)}, \alpha_{i+1}^{(2)} \right)
\end{aligned}$$

It is possible now to evaluate the 'viscous' terms:

- *Evaluation of conservative terms*

$$\begin{aligned}
\mathcal{E} \left(X(x_{i+1/2}, t) F_v(U_{i+1/2}^*) \right) &= P_{1+1/2}(\Sigma_1 - \Sigma_1) F_v(U_i^{(1)}, U_{i+1}^{(1)}) \\
&+ P_{1+1/2}(\Sigma_1 - \Sigma_2) \left(\beta_{i+1/2}^{(1,2)} \right)^+ F_v(U_i^{(1)}, U_{i+1}^{(2)}) + \\
&+ P_{1+1/2}(\Sigma_2 - \Sigma_1) \left(-\beta_{i+1/2}^{(2,1)} \right)^+ F_v(U_i^{(2)}, U_{i+1}^{(1)})
\end{aligned}$$

$$\begin{aligned}
\mathcal{E} \left(X(x_{i-1/2}, t) F_v(U_{i-1/2}^*) \right) &= P_{1-1/2}(\Sigma_1, \Sigma_1) F_v(U_{i-1}^{(1)}, U_i^{(1)}) \\
&+ P_{1-1/2}(\Sigma_1, \Sigma_2) \left(\beta_{i-1/2}^{(1,2)} \right)^+ F_v(U_{i-1}^{(1)}, U_i^{(2)}) + \\
&+ P_{1-1/2}(\Sigma_2, \Sigma_1) \left(-\beta_{i-1/2}^{(2,1)} \right)^+ F_v(U_{i-1}^{(2)}, U_i^{(1)}).
\end{aligned}$$

- *Evaluation of non-conservative terms*

$$\begin{aligned}
& \mathcal{E} \left([X]_{N(w)} F_{vI}(U_i^{N(w)}, U_{i+1}^-) \right) = \\
& = P_{1+1/2}(\Sigma_1, \Sigma_2) \left(\beta_{i+1/2}^{(1,2)} \right)^- F_{vI}(U_i^{(1)}, U_{i+1}^{(2)}) + \\
& \quad - P_{1+1/2}(\Sigma_2, \Sigma_1) \left(\beta_{i+1/2}^{(2,1)} \right)^- F_{vI}(U_i^{(2)}, U_{i+1}^{(1)}) \\
& \mathcal{E} \left([X]_0 F_{vI}(U_{i-1}^+, U_i^0) \right) = \\
& = -P_{1-1/2}(\Sigma_1, \Sigma_2) \left(\beta_{i-1/2}^{(1,2)} \right)^+ F_{vI}(U_{i-1}^{(1)}, U_i^{(2)}) + \\
& \quad + P_{1-1/2}(\Sigma_2, \Sigma_1) \left(\beta_{i-1/2}^{(2,1)} \right)^+ F_{vI}(U_{i-1}^{(2)}, U_i^{(1)}).
\end{aligned}$$

- *Relaxations terms*

$$\mathcal{E} \left(\frac{N(\omega)_{int}}{\Delta x} \right) ((F_v(U_i^2, U_i^1) - F_v(U_i^1, U_i^2))) = \lambda_i (F_v(U_i^2, U_i^1) - F_v(U_i^1, U_i^2))$$

Compared to the Euler equations, the presence of the viscosity transforms the conservation laws of momentum and energy into second-order partial differential equations (see Eq. 10-11). Thus, the viscous fluxes F_v and F_{vI} are reconstructed by a forward difference. We consider, for example, the cell boundary $i + 1/2$ and we define thus in the case of momentum and energy equation:

- *momentum*

$$F_v(U_i^{(k)}, U_{i+1}^{(k)}) = \begin{cases} \frac{4}{3}\mu \frac{u_{i+1}^{(k)} - u_i^{(k)}}{dx} & \text{if flux direction is } \rightarrow \\ \frac{4}{3}\mu \frac{u_i^{(k)} - u_{i+1}^{(k)}}{dx} & \text{if flux direction is } \leftarrow \end{cases}$$

- *energy*

$$F_v(U_i^{(k)}, U_{i+1}^{(k)}) = \begin{cases} \frac{4}{3}\mu u_{i+\frac{1}{2}} \frac{u_{i+1}^{(k)} - u_i^{(k)}}{dx} & \text{if flux direction is } \rightarrow \\ \frac{4}{3}\mu u_{i+\frac{1}{2}} \frac{u_i^{(k)} - u_{i+1}^{(k)}}{dx} & \text{if flux direction is } \leftarrow \end{cases}$$

(22)

- *momentum*

$$F_{vI}(U_i^{(k)}, U_{i+1}^{(k)}) = \begin{cases} \frac{4}{3}\mu \frac{u_{I_{i+1}}^{(k)} - u_{I_i}^{(k)}}{dx} & \text{if flux direction is } \rightarrow \\ \frac{4}{3}\mu \frac{u_{I_i}^{(k)} - u_{I_{i+1}}^{(k)}}{dx} & \text{if flux direction is } \leftarrow \end{cases}$$

- *energy*

$$F_{vI}(U_i^{(k)}, U_{i+1}^{(k)}) = \begin{cases} \frac{4}{3}\mu u_{I_{i+\frac{1}{2}}} \frac{u_{I_{i+1}}^{(k)} - u_{I_i}^{(k)}}{dx} & \text{if flux direction is } \rightarrow \\ \frac{4}{3}\mu u_{I_{i+\frac{1}{2}}} \frac{u_{I_i}^{(k)} - u_{I_{i+1}}^{(k)}}{dx} & \text{if flux direction is } \leftarrow \end{cases}$$

(23)

where $u_{i+\frac{1}{2}}$ and $u_{I_{i+\frac{1}{2}}}$ are, respectively, the phase velocity and the interface velocity determined by Riemann solver.

Flow Patterns	Left and Right States	Flux Indicator
Σ_1, Σ_2	$F_v(U_i^{(1)}, U_{i+1}^{(2)})$	$\left(\beta_{i+1/2}^{(1,2)}\right)^+$
Σ_1, Σ_1	$F_v(U_i^{(1)}, U_{i+1}^{(1)})$	1
Σ_2, Σ_1	$F_v(U_i^{(2)}, U_{i+1}^{(1)})$	$-\left(\beta_{i+1/2}^{(2,1)}\right)^+$
Σ_2, Σ_2	$F_v(U_i^{(2)}, U_{i+1}^{(2)})$	0
Interface Viscous Flux		
$\Sigma_1 - \Sigma_2$	$F_{v_I}(U_i^{(1)}, U_{i+1}^{(2)})$	$\left(\beta_{i+1/2}^{(1,2)}\right)^+$
$\Sigma_1 - \Sigma_1$	$F_{v_I}(U_i^{(1)}, U_{i+1}^{(1)})$	0
$\Sigma_2 - \Sigma_1$	$F_{v_I}(U_i^{(2)}, U_{i+1}^{(1)})$	$-\left(\beta_{i+1/2}^{(2,1)}\right)^+$
$\Sigma_2 - \Sigma_2$	$F_{v_I}(U_i^{(2)}, U_{i+1}^{(2)})$	0

Table 1: The various flow configurations at cell boundary $i + 1/2$.

3.2 Second-Order accuracy

Following the MUSCL approach, we propose an extension to a second-order approximation of the scheme:

$$\begin{aligned}
& \frac{\left(\alpha_i^{(1)} U_i^{(1)}\right)^{n+1} - \left(\alpha_i^{(1)} U_i^{(1)}\right)^n}{\Delta t} \\
& + \frac{\mathcal{E}(XF)_{i+1/2} - \mathcal{E}(XF)_{i-1/2}}{\Delta x} - \frac{\mathcal{E}(XF_v)_{i+1/2} - \mathcal{E}(XF_v)_{i-1/2}}{\Delta x} = \\
& = \mathcal{E}\left(F^{lag} \frac{\partial X}{\partial x}\right)_{i,bound} + \mathcal{E}\left(F^{lag} \frac{\partial X}{\partial x}\right)_{i,relax} + \\
& - \mathcal{E}\left(F_v \frac{\partial X}{\partial x}\right)_{i,bound} - \mathcal{E}\left(F_v \frac{\partial X}{\partial x}\right)_{i,relax} \tag{24}
\end{aligned}$$

As in section 3.1, we write explicitly only the terms that are not developed in [7, 11]. In the following, $U_{i\pm 1/2,l}$ (resp. $U_{i\pm 1/2,r}$) are the vector of conservative variables on the left (resp. right) of the boundary cell $x_{i\pm 1/2}$ after the MUSCL extrapolation, using a *minmod* limiter. Thus, the viscous terms in the predictor-corrector scheme for a multiphase flows, take the following form

- *Evaluation of conservative terms*

$$\begin{aligned}
\mathcal{E}(XF_v)_{i+1/2} & = P_{1+1/2}(\Sigma_1, \Sigma_1) F_v(U_{i+1/2,l}^{(1)}, U_{i+1/2,r}^{(1)}) \\
& + P_{1+1/2}(\Sigma_1, \Sigma_2) \left(\beta_{i+1/2}^{(1,2)}\right)^+ F_v(U_{i+1/2,l}^{(1)}, U_{i+1/2,r}^{(2)}) + \\
& + P_{1+1/2}(\Sigma_2, \Sigma_1) \left(-\beta_{i+1/2}^{(2,1)}\right)^+ F_v(U_{i+1/2,l}^{(2)}, U_{i+1/2,r}^{(1)}) \tag{25}
\end{aligned}$$

$$\begin{aligned}
 \mathcal{E}(XF_v)_{i-1/2} &= P_{1-1/2}(\Sigma_1, \Sigma_1) F_v(U_{i-1/2,l}^{(1)}, U_{i-1/2,r}^{(1)}) \\
 &+ P_{1-1/2}(\Sigma_1, \Sigma_2) \left(\beta_{i-1/2}^{(1,2)} \right)^+ F_v(U_{i-1/2,l}^{(1)}, U_{i-1/2,r}^{(2)}) + \\
 &+ P_{1-1/2}(\Sigma_2, \Sigma_1) \left(-\beta_{i-1/2}^{(2,1)} \right)^+ F_v(U_{i-1/2,l}^{(2)}, U_{i-1/2,r}^{(1)})
 \end{aligned} \tag{26}$$

- *Evaluation of non-conservative terms*

$$\begin{aligned}
 \mathcal{E} \left(F_v \frac{\partial X}{\partial x} \right)_i &= \mathcal{E} \left(F_v \frac{\partial X}{\partial x} \right)_{bound} + \mathcal{E} \left(F_v \frac{\partial X}{\partial x} \right)_{relax} = \\
 &= P_{1+1/2}(\Sigma_1, \Sigma_2) \left(\beta_{i+1/2}^{(1,2)} \right)^- F_{vI}(U_{i+1/2,l}^{(1)}, U_{i+1/2,r}^{(2)}) + \\
 &- P_{1+1/2}(\Sigma_2, \Sigma_1) \left(\beta_{i+1/2}^{(2,1)} \right)^- F_{vI}(U_{i+1/2,l}^{(2)}, U_{i+1/2,r}^{(1)}) + \\
 &- P_{1-1/2}(\Sigma_1, \Sigma_2) \left(\beta_{i-1/2}^{(1,2)} \right)^+ F_{vI}(U_{i-1/2,l}^{(1)}, U_{i-1/2,r}^{(2)}) + \\
 &+ P_{1-1/2}(\Sigma_2, \Sigma_1) \left(\beta_{i-1/2}^{(2,1)} \right)^+ F_{vI}(U_{i-1/2,l}^{(2)}, U_{i-1/2,r}^{(1)}) + \\
 &+ \max(0, \Delta\alpha_i^1) (F_v(U_i^2, U_i^1) - \max(0, \Delta\alpha_i^2) F_v(U_i^1, U_i^2)),
 \end{aligned} \tag{27}$$

where $\Delta\alpha_i^1 = \alpha_{i+1/2,l}^1 - \alpha_{i+1/2,r}^1$ and $\Delta\alpha_i^2 = \alpha_{i+1/2,l}^2 - \alpha_{i+1/2,r}^2$ are the limited slope of α^1 and α^2 in the cell C_i . The viscous fluxes F_v and F_{vI} are reconstructed by a backward difference on the base of flow direction. We consider the cell boundary $i+1/2$ and the viscous fluxes for the momentum and energy equations are:

- *momentum*

$$F_v(U_{i+1/2,l}^{(k)}, U_{i+1/2,r}^{(k)}) = \begin{cases} \frac{4}{3}\mu \frac{u_{i+\frac{1}{2}} - u_{i-1}^{(k)}}{(3/2)dx} & \text{if flux direction is } \rightarrow \\ \frac{4}{3}\mu \frac{u_{i+\frac{1}{2}} - u_{i+2}^{(k)}}{(3/2)dx} & \text{if flux direction is } \leftarrow \end{cases}$$

- *energy*

$$F_v(U_{i+1/2,l}^{(k)}, U_{i+1/2,r}^{(k)}) = \begin{cases} \frac{4}{3}\mu u_{i+\frac{1}{2}} \frac{u_{i+\frac{1}{2}} - u_{i-1}^{(k)}}{(3/2)dx} & \text{if flux direction is } \rightarrow \\ \frac{4}{3}\mu u_{i+\frac{1}{2}} \frac{u_{i+\frac{1}{2}} - u_{i+2}^{(k)}}{3/2dx} & \text{if flux direction is } \leftarrow \end{cases} \tag{28}$$

- *momentum*

$$F_{vI}(U_{i+1/2,l}^{(k)}, U_{i+1/2,r}^{(k)}) = \begin{cases} \frac{4}{3}\mu \frac{u_{I(r)i+1}^{(k)} - u_{I(r)i}^{(k)}}{dx} & \text{if flux direction is } \rightarrow \\ \frac{4}{3}\mu \frac{u_{I(r)i}^{(k)} - u_{I(r)i+1}^{(k)}}{dx} & \text{if flux direction is } \leftarrow \end{cases}$$

- *energy*

$$F_{vI}(U_{i+1/2,l}^{(k)}, U_{i+1/2,r}^{(k)}) = \begin{cases} \frac{4}{3}\mu u_{I+\frac{1}{2}}^{(k)} \frac{u_{I(r)i+1}^{(k)} - u_{I(r)i}^{(k)}}{dx} & \text{if flux direction is } \rightarrow \\ \frac{4}{3}\mu u_{I+\frac{1}{2}}^{(k)} \frac{u_{I(r)i}^{(k)} - u_{I(r)i+1}^{(k)}}{dx} & \text{if flux direction is } \leftarrow \end{cases} \tag{29}$$

where

$$\begin{aligned} u_{i+\frac{1}{2}}^{(k)} &= \begin{cases} u_{(d)_i}^{(k)} & \text{if flux direction is } \rightarrow \\ u_{(l)_{i+1}}^{(k)} & \text{if flux direction is } \leftarrow \end{cases} \\ u_{I_{i+\frac{1}{2}}}^{(k)} &= \begin{cases} u_{(d)_{I_i}}^{(k)} & \text{if flux direction is } \rightarrow \\ u_{(l)_{I_{i+1}}}^{(k)} & \text{if flux direction is } \leftarrow \end{cases} \end{aligned} \quad (30)$$

where l and r represent the left and right side.

In order to obtain the predictor scheme, the solution is calculated at time $t = n + 1/2$ and in the corrector scheme the solution is calculated at time $t = n + 1$, using the solution computed at the predictor step.

4 Asymptotic analysis of the numerical scheme

The earlier presented scheme (Eq.24) is a semi-discrete numerical approximation of the seven equation model for the modelization of a two-phase flow. An asymptotic expansion of the scheme using the procedure proposed by Abgrall and Perrier [11] is developed. The aim is to obtain the semi-discrete scheme for the modelization of a reduced five equations model in a 1D configuration, where viscous effects considered. If we set $\varepsilon_i = 1/\lambda_i$, the discrete scheme for the seven equations model can be formally rewritten as

$$\frac{\partial W}{\partial t} + \frac{G}{\Delta x} = \frac{R(W)}{\varepsilon_i}. \quad (31)$$

where $W = (\alpha^{(1)}, \alpha^{(1)}U^{(1)}, \alpha^{(2)}, \alpha^{(2)}U^{(2)})$, G is the sum of convective fluxes, viscous fluxes and *bound* lagrangian fluxes, moreover $R(W)$ are the relaxation terms.

Before developing the asymptotic expansion, it is necessary to remark that for the Laplace law, we know the relation between the difference of phases pressure P , the stress tensor \bar{T} and the surface tension σ . In particular, according to the normal flow, we have:

$$P_1 - P_2 + \mathbb{T} \cdot n = 2H\sigma, \quad (32)$$

where H is the curvature of interface. In 1D dimension $H = 0$ and, moreover, we know that in the hypothesis of relaxation, we consider that in the cell the velocity and pressure of the two phases are the same, *i.e.* (only into the cell) $P_1 = P_2$. So, the Eq. 32 reduces to $\mathbb{T} \cdot n = 0$ and thus the viscous relaxation terms disappears from Eq. 24.

As a consequence, the procedure of asymptotic expansion is the same developed for the Eulerian scheme as in [11, 9]. Let us consider $\varepsilon \rightarrow 0$ and we look for the solutions such that the relaxation terms disappear:

$$\mathcal{W} = \left\{ W \text{ such that } R(W) = 0 \Rightarrow \mathcal{E} \left(F^{lag} \frac{\partial X}{\partial x} \right)_{i,relax} = 0 \right\} \quad (33)$$

For each solution W , it exists a parameterization M such that: $M : u \rightarrow M(u)$, in which u are the primitive variables of vector W . Let us consider the solutions

of the form:

$$W = M(u) + \varepsilon V \quad (34)$$

where V is a neighborhood of W in \mathcal{W} and we can obtain an expansion of the form:

$$R(W) = R(M(u)) + \varepsilon R'(M(u))V + o(\varepsilon) \quad (35)$$

We denote with $dM_u = \{dM_u^1, \dots, dM_u^n\}$ the Jacobian matrix such that its column vectors form a basis of $\ker R'(M(u))$ (see [9] for details), with $\{I^1, \dots, I^{N-n}\}$ a basis of $\text{Rng}(R'(M(u)))$ that is the range of $R'(M(u))$ and with P the projection on $\ker R'(M(u))$ in the direction of $\text{Rng}(R'(M(u)))$. Let P be equal to the inverse of matrix $S = [dM_u^1, \dots, dM_u^n, I^1, I^2]$. We replace the Eq.(34) and Eq.(35) into the Eq.(31) and we multiply it for the projection P ,

$$PdM_u \frac{\partial u}{\partial t} + P \frac{\partial G}{\partial \Delta x} = PR'(M(u)). \quad (36)$$

Let us remember that the product $P \times dM_u = Id(n)$ where $Id(n)$ is a $n \times n$ identity matrix and that the product $P \times R'(M(u)) = 0$, thus, Eq.(36) represents the reduced semi-discrete scheme.

4.1 Scheme for the reduced model including viscous effect

Following the procedure described into the section 4, in order to obtain the reduced scheme (36), it is necessary to define:

- the parameterization M that allows defining the Jacobian matrix dM_u ;
- a basis of the range $\text{Rng}(R'(M(u)))$ to obtain the vector I^1 and I^2 ;
- the inverse matrix of S that allows calculating the projector P .

Let $u = \{\alpha_1, \rho_1, u, P, \alpha_2, \rho_2\}$ the vector of primitives variables, thus the mapping $M : u \rightarrow M(u)$ is:

$$M : \begin{pmatrix} \alpha_1 \\ \rho_1 \\ u \\ P \\ \alpha_2 \\ \rho_2 \end{pmatrix} \rightarrow \begin{pmatrix} \alpha_1 \\ \rho_1 \\ u \\ P \\ \alpha_2 \\ \rho_2 \\ u \\ P \end{pmatrix}$$

and thus the Jacobian matrix is:

$$dM_u = \begin{pmatrix} 1 & 0 & 0 & 0 & 0 & 0 \\ 0 & 1 & 0 & 0 & 0 & 0 \\ 0 & 0 & 1 & 0 & 0 & 0 \\ 0 & 0 & 0 & 1 & 0 & 0 \\ 0 & 0 & 0 & 0 & 1 & 0 \\ 0 & 0 & 0 & 0 & 0 & 1 \\ 0 & 0 & 1 & 0 & 0 & 0 \\ 0 & 0 & 0 & 1 & 0 & 0 \end{pmatrix}.$$

To obtain the reduced scheme it is necessary to provide the form of the numerical scheme for the seven equations model in primitive variables. The system (31) can be written in the following simplified version:

$$\begin{cases} \frac{\partial \bar{\alpha}_i^k}{\partial t} = V F_i^k \\ \frac{\partial \bar{\alpha}_i^k \bar{\rho}_i^k}{\partial t} = M_a F_i^k \\ \frac{\partial \bar{\alpha}_i^k \bar{\rho}_i^k u_i^k}{\partial t} = M_o F_i^k \\ \frac{\partial \bar{\alpha}_i^k \bar{\rho}_i^k \bar{E}_i^k}{\partial t} = E F_i^k \end{cases}$$

After several manipulation, as in [11], allows obtaining the system of seven equations in non-conservatives variables:

$$\begin{cases} \frac{\partial \bar{\alpha}_i^k}{\partial t} = V F_i^k \\ \bar{\alpha}_i^k \frac{\partial \bar{\rho}_i^k}{\partial t} = M_a F_i^k - \bar{\rho}_i^k V F_i^k \\ \bar{\alpha}_i^k \bar{\rho}_i^k \frac{\partial u_i^k}{\partial t} = M_o F_i^k \\ \frac{\partial \bar{E}_i^k}{\partial t} = \frac{E F_i^k}{\bar{\alpha}_i^k \bar{\rho}_i^k \beta_i^k} - \frac{u_i^k M_o F_i^k}{\bar{\alpha}_i^k \bar{\rho}_i^k \beta_i^k} + \frac{u_i^{k2}}{2} - \varepsilon_i^k - \rho_i^k \kappa_i^k M_a F_i^k + \frac{\rho_i^{k2} \kappa_i^k V F_i^k}{\bar{\alpha}_i^k \bar{\rho}_i^k \beta_i^k} \end{cases} \quad (37)$$

where

$$\beta_i^k = \left(\frac{\partial \varepsilon_i^k}{\partial P_i^k} \right)_{\rho_i^k} \quad \text{and} \quad \kappa_i^k = \left(\frac{\partial \varepsilon_i^k}{\partial \rho_i^k} \right)_{P_i^k}$$

The system (37) can be written as:

$$\frac{\partial U}{\partial t} + \frac{G(U)}{\Delta x} = T \frac{R(U)}{\varepsilon_i} \quad (38)$$

where U is the vector of primitive variables and T is a linear transformation between primitive and conservative variables:

$$T = \begin{pmatrix} T_1 & 0 \\ 0 & T_2 \end{pmatrix},$$

with

$$T_i = \begin{pmatrix} 1 & 0 & 0 & 0 \\ -\frac{\rho_i}{\alpha_i} & \frac{1}{\alpha_i} & 0 & 0 \\ 0 & -\frac{u_i}{\alpha_i \rho_i} & \frac{1}{\alpha_i \rho_i} & 0 \\ \frac{\kappa_i \rho_i^2}{\bar{\alpha}_i^k \bar{\rho}_i^k \beta_i^k} & \frac{u_i^{k2}}{2} - \varepsilon_i^k - \rho_i^k \kappa_i^k}{\bar{\alpha}_i^k \bar{\rho}_i^k \beta_i^k} & -\frac{u_i^k}{\bar{\alpha}_i^k \bar{\rho}_i^k \beta_i^k} & \frac{1}{\bar{\alpha}_i^k \bar{\rho}_i^k \beta_i^k} \end{pmatrix}.$$

Now, it is possible to determine the basis of the vectors I^1 and I^2 , knowing that the matrix $R'(M(u))$ is the product between the matrix T and the matrix in

which each term is the derivative of $(F^{lag}(U^1, U^2) - F^{lag}(U^2, U^1))$ with respect to primitive variables:

$$R'(M_u) = \begin{pmatrix} 0 & 0 & 0 & -\lambda & 0 & 0 & 0 & \lambda \\ 0 & 0 & 0 & \lambda \frac{\rho_1}{\alpha_1} & 0 & 0 & 0 & -\lambda \frac{\rho_1}{\alpha_1} \\ 0 & 0 & \mu \frac{1}{\alpha_1 \rho_1} & 0 & 0 & 0 & \mu \frac{1}{\alpha_1 \rho_1} & 0 \\ 0 & 0 & 0 & \lambda \left(-\frac{\kappa_1 \rho_1^2}{\alpha_1 \rho_1 \beta_1} + \frac{P}{\alpha_1 \rho_1 \beta_1} \right) & 0 & 0 & 0 & \lambda \left(\frac{\kappa_1 \rho_1^2}{\alpha_1 \rho_1 \beta_1} - \frac{P}{\alpha_1 \rho_1 \beta_1} \right) \\ 0 & 0 & 0 & -\lambda & 0 & 0 & 0 & \lambda \\ 0 & 0 & 0 & \lambda \frac{\rho_2}{\alpha_2} & 0 & 0 & 0 & -\lambda \frac{\rho_2}{\alpha_2} \\ 0 & 0 & \mu \frac{1}{\alpha_2 \rho_2} & 0 & 0 & 0 & \mu \frac{1}{\alpha_2 \rho_2} & 0 \\ 0 & 0 & 0 & \lambda \left(-\frac{\kappa_2 \rho_2^2}{\alpha_2 \rho_2 \beta_2} + \frac{P}{\alpha_2 \rho_2 \beta_2} \right) & 0 & 0 & 0 & \lambda \left(\frac{\kappa_2 \rho_2^2}{\alpha_2 \rho_2 \beta_2} - \frac{P}{\alpha_2 \rho_2 \beta_2} \right) \end{pmatrix}.$$

A basis of the range $Rng(R'(M(u)))$ is the set:

$$I^1 = \begin{pmatrix} 1 \\ -\frac{\rho_1}{\alpha_1} \\ 0 \\ \frac{a_1^2 \rho_1}{\alpha_1} \\ -1 \\ \frac{\rho_2}{\alpha_2} \\ 0 \\ \frac{a_2^2 \rho_2}{\alpha_2} \end{pmatrix}; \quad I^2 = \begin{pmatrix} 0 \\ 0 \\ \frac{1}{\alpha_1 \rho_1} \\ 0 \\ 0 \\ 0 \\ -\frac{1}{\alpha_2 \rho_2} \\ 0 \end{pmatrix}.$$

Finally, the inversion of the matrix $S = [dM_u^1, \dots, dM_u^6, I^1, I^2]$ gives the matrix of projector:

$$P = \begin{pmatrix} 1 & 0 & 0 & \frac{\alpha_1 \alpha_2}{d} & 0 & 0 & 0 & -\frac{\alpha_1 \alpha_2}{d} \\ 0 & 1 & 0 & -\frac{\alpha_2 \rho_1}{d} & 0 & 0 & 0 & \frac{\alpha_2 \rho_1}{d} \\ 0 & 0 & \frac{\alpha_1 \rho_1}{\alpha_1 \rho_1 + \alpha_2 \rho_2} & 0 & 0 & 0 & \frac{\alpha_2 \rho_2}{\alpha_1 \rho_1 + \alpha_2 \rho_2} & 0 \\ 0 & 0 & 0 & \frac{\alpha_1 \rho_2 a_2^2}{d} & 0 & 0 & 0 & -\frac{\alpha_2 \rho_1 a_1^2}{d} \\ 0 & 0 & 0 & -\frac{\alpha_1 \alpha_2}{d} & 1 & 0 & 0 & \frac{\alpha_1 \alpha_2}{d} \\ 0 & 0 & 0 & \frac{\alpha_1 \rho_2}{d} & 0 & 0 & 0 & -\frac{\alpha_1 \rho_2}{d} \end{pmatrix},$$

with $d = \alpha_1 \rho^2 (a_2)^2 + \alpha_2 \rho^1 (a_1)^2$ and $a_k^2 = \frac{P_k - \kappa_k \rho_k^2}{\beta_k \rho_k^2}$. Now, it is possible to obtain the final scheme for the five equation model in conservative variables :

$$\left\{ \begin{array}{l} \frac{\partial \bar{\alpha}_2}{\partial t} = FV_2 + \frac{\bar{\alpha}_1 \bar{\alpha}_2}{\bar{\alpha}_2 \bar{\rho}_1 a_1^2 + \bar{\alpha}_1 \bar{\rho}_2 a_2^2} \left\{ \frac{SE_2}{\bar{\alpha}_2 \bar{\rho}_2 \beta_2} - \frac{u_2 SU_2}{\bar{\alpha}_2 \bar{\rho}_2 \beta_2} + \frac{\frac{u_2^2}{2} - \varepsilon_2 - \rho_2 \kappa_2}{\bar{\alpha}_2 \bar{\rho}_2 \beta_2} M_2 + \right. \\ \left. \frac{\rho_2^2 \kappa_2 FV_2}{\bar{\alpha}_2 \bar{\rho}_2 \beta_2} - \frac{SE_1}{\bar{\alpha}_1 \bar{\rho}_1 \beta_1} + \frac{u_1 SU_1}{\bar{\alpha}_1 \bar{\rho}_1 \beta_1} - \frac{\frac{u_1^2}{2} - \varepsilon_1 - \rho_1 \kappa_1}{\bar{\alpha}_1 \bar{\rho}_1 \beta_1} M_1 - \frac{\rho_1^2 \kappa_1 FV_1}{\bar{\alpha}_1 \bar{\rho}_1 \beta_1} \right\} \\ \frac{\partial \alpha_k \bar{\rho}_k}{\partial t} = M_k \\ \frac{\partial \rho u}{\partial t} = SU_1 + SU_2 \\ \frac{\partial \rho E}{\partial t} = SE_1 + SE_2 \end{array} \right. \quad (39)$$

Air	Water
$\gamma = 1.4$	$\gamma = 4.4$
$P_\infty = 0Pa$	$P_\infty = 6 \times 10^8 Pa$

Table 2: EOS coefficient for air and water

5 Thermodynamic Closure

We consider a Stiffened Gas (EOS) to describe both liquid and gas:

$$\rho e = \frac{(P + \gamma P_\infty)}{\gamma - 1}$$

where e is the internal energy, p is the phase pressure, γ and P_∞ are two constants characteristic of each fluid. In this work, the fluid used are air (at $T=293,25$ K and $T=410.52$ K) and water (at room conditions). The constants for these fluids are summarized in Table2.

6 Results

The aim of this section is to highlight the capabilities of the proposed scheme for the numerical resolution of interface problems with viscous effects.

This section is divided in two parts: (i) in the first one, the code validation is presented, displaying a set of test cases where the effects of viscosity are significant; (ii) in the last one, the results obtained by solving the Navier-Stokes equations are compared to the Euler solutions on some test-cases well-known in literature. Remark that each run has been made with a CFL number equal to 0.6 by using the Relaxation solver introduced in the previous section.

6.1 Validation

Three test cases in a shock-tube configuration have been selected for the code validation. The first case has been created in order to evaluate the presence of viscous effects in a monophasic region, that is generally hard to appreciate for water at standard conditions. Then, an artificial fluid has been taken into account, that has the same properties of water at standard condition, except for the viscosity, assumed 10^6 times more elevated than the that one of water. In the second test-case, a bi-phase flow is simulated with the same fluid of the first test-case and the air. Finally, the code has been validated on a test-case known in literature [1].

6.1.1 One fluid test-case with very high viscosity

It is known in literature that in a compressible 1D simulation, the difference between a viscous and a Euler simulation can be observed, for example, around a shock-wave (see Fig.3) in particular conditions. As shown in Liepmann and Roshko [15] (see also [13]), it is possible to evaluate the order of magnitude of shock-wave thickness Δx knowing the velocity jump across the shock $[u]$ and

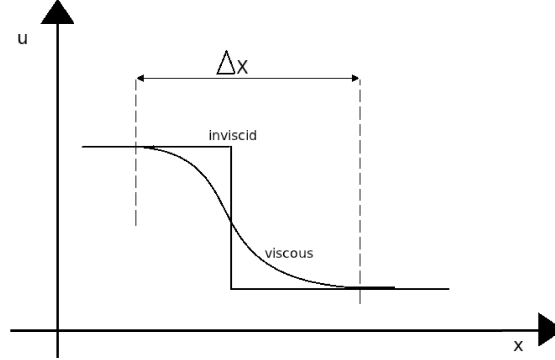


Figure 3: Development of a viscous transition compared to inviscid transition of a discontinuity.

the kinematic viscosity $\nu = \mu/\rho$:

$$\Delta x \approx \frac{\nu}{[u]}. \quad (40)$$

Let us estimate the shock-wave thickness developed in a shock tube, filled with water at standard condition, for which a velocity jump $[u] = 230m$ is generated (test case already analyzed in [7]). For Eq.(40), the thickness Δx is proportional to $10^{-9}m$. Thus, this means that in order to observe the difference between a viscous or an inviscid simulation, one should use a mesh of 10^9 points.

For that reason, we supposed to use a fluid with the same properties of water at standard condition, but with a viscosity equal to $\mu = 2300Pa \cdot s$, so that the the shock-wave thickness should be of the order of $\Delta x = 0.01m$.

The shock tube is filled out with only one fluid. At the beginning, both side of the tube are at rest, the left side is at a pressure of $10^9 Pa$, while the right one at a pressure of $10^5 Pa$. The diaphragm is located at $x=0.5m$ and the second-order scheme has been used.

If a mesh of 100 points is used, some difference of the velocity profiles (the profiles are obtained at $t=150\mu s$) can be observed between the viscous and inviscid solution (see Fig.4(a)). In this case, the effect of viscosity produces a round shock transition, unlike the sharp shock transition produced by an inviscid computation. This difference is more evident with a finer mesh (see Fig.4(a)).

6.1.2 Two-fluids test-case with very high viscosities

Let us suppose, now, to have the same condition of pressure of the previous test case, but to consider two fluids, with the same volume fraction ($\alpha_k = 0.5$) on the right and on the left of diaphragm, located at $x=0.5m$.

Let us suppose also that the two fluids have the same properties of water and air at standard conditions except for the viscosity modified on the base of shock-wave thickness, as already shown in section 6.1.1.

In a two-phase problem, the Eq.(40) can not be applied in its original form. Now, the problem is to compute the *artificial* viscosity to use in order to appreciate viscous effects. Then, the thickness has been assumed equal to $\Delta x = 0.001$,

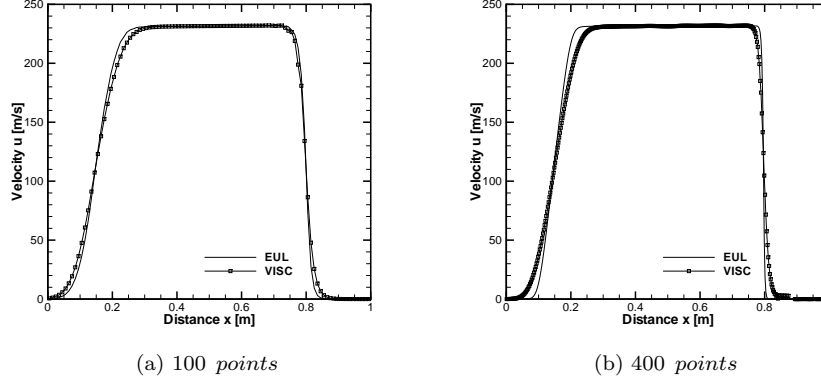


Figure 4: Comparison of Euler and viscous velocity profiles obtained with different meshes.

and the associated viscosity for each fluid has been computed by considering like that the tube is filled out with a single fluid. The viscosities are computed as follows:

$$\begin{aligned}
 & - \text{Water} \\
 & \begin{cases} \Delta x = 0.001 \text{ m} \\ \rho = 1000 \frac{\text{kg}}{\text{m}^3} \end{cases} \rightarrow \mu = 630 \text{ Pa} \cdot \text{s}, \\
 & - \text{Air} \\
 & \begin{cases} \Delta x = 0.001 \text{ m} \\ \rho = 50 \frac{\text{kg}}{\text{m}^3} \end{cases} \rightarrow \mu = 31.5 \text{ Pa} \cdot \text{s}.
 \end{aligned}$$

At these conditions, a mesh of 1000 points has been used and the inviscid and viscous solutions have been compared. As it can be observed in Fig.(5), also in the two-phase problem, the viscous solution differs from the Euler one. The velocity profiles between inviscid and viscous computations are very similar. The density and volume fraction profiles (Fig.(5)) display a maximal difference of 50% and 5%, respectively.

6.1.3 Surana [1] viscous test-case with air

The results obtained in [1] have been compared to the results obtained with the presented scheme. Surana used a Navier-Stokes equations in a 1D single-phase flow simulation. The shock tube is filled out with air with the following properties:

$$\begin{aligned}
 \hat{\rho} &= 1.225 \text{ kg/m}^3 & \hat{\mu} &= 0.198 \times 10^{-4} \text{ Pa} \cdot \text{s} \\
 \hat{T} &= 410.52 \text{ K} & Re &= 31.891
 \end{aligned}$$

At time $t=0$ the following reference values are used:

$$\begin{aligned}
 t_0 &= 0.454479 \times 10^{-8} \text{ s} & \hat{P}_l &= 1.44323 \times 10^5 \text{ Pa} \\
 L_0 &= 0.156 \times 10^{-5} \text{ m} & \hat{P}_h &= 2.88647 \times 10^6 \text{ Pa} \\
 u_0 &= 343.25 \text{ m/s} & \rho_h / \rho_l &= 20
 \end{aligned}$$

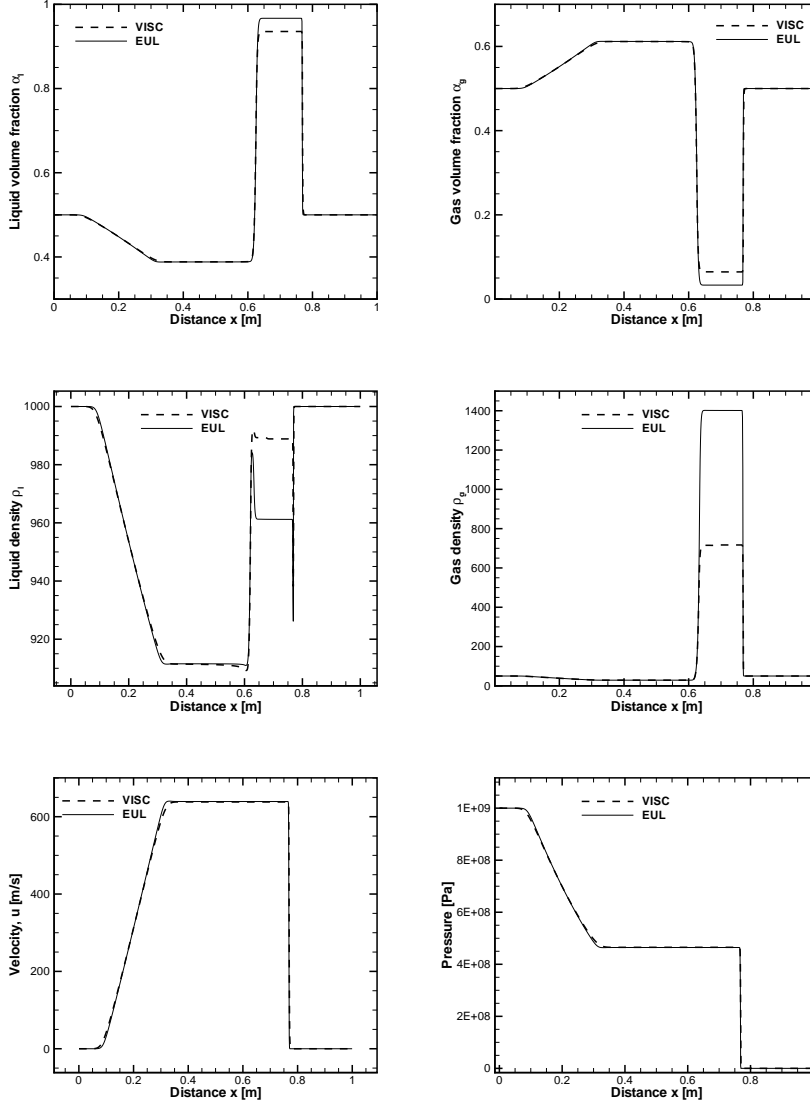


Figure 5: Comparison of Euler and Viscous computations.

Both sides of the tube are at rest, the left side is at a low pressure equal to P_l while the right side is at an higher pressure equal to P_h . The tube length is $L = \hat{L}/L_0 = 2$ and the diaphragm is located at $\hat{L} = 0.156 \times 10^{-5}m$. The same uniform grid mesh of 102 points as in [1] is used. From the analysis of density and velocity profiles we can observe a good agreement with the numerical results obtained by Surana [1] (Fig.6-7). In particular, for the velocity, a very good agreement is obtained at a time $t = 0.9089 \times 10^{-10}s$ and $t = 0.1636 \times 10^{-8}s$ (Fig.6(a),(c)), while at time $t = 0.1818 \times 10^{-9}s$ the minimal value of velocity estimated with the present scheme is 4% higher than Surana result (Fig.6(b)). For the density, a very good agreement is obtained in the first and second time-

step (Fig.7(a),(b)), while in the eighteenth time-step, between $0.2 < x < 0.7$, the two profiles display some differences, even if they present the same trend (Fig.7(c)).

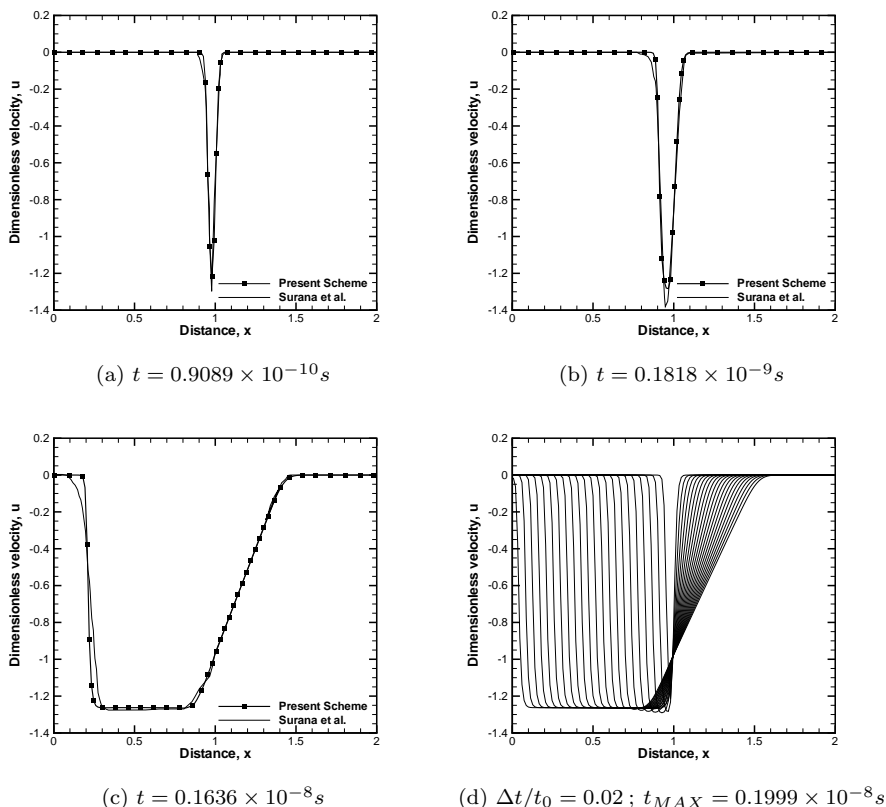


Figure 6: In (a), (b) and (c): comparison of velocity profiles u obtained by Surana *et al.* [1] and by DEM, respectively in the first, second and eighteenth time-step. (d) Evolution of velocity obtained with DEM.

6.2 Shock-tube with water

In this case, the shock tube is filled out with water only. At the beginning, both sides of the tube are at rest, the left side is at a pressure of 10^9 Pa, while the right one is at a pressure of 10^5 Pa. The diaphragm is located at $x=0.5$ m and the profiles shown in the following figures are all taken at a $t=150\mu s$. A 1000 points mesh has been used. The second order scheme has been used.

The results obtained with an Eulerian formulation are compared to those ones obtained considering viscous effects. In Fig.8, it can be observed that there are not remarkable differences between the two computations.

Computing the thickness shock wave (see Eq.(40)), for this case ($\Delta x \approx \times^{-9}$), we conclude that the difference between the two computations cannot be observed with the used mesh. As a consequence, shock can be treated in the same way as in inviscid flows.

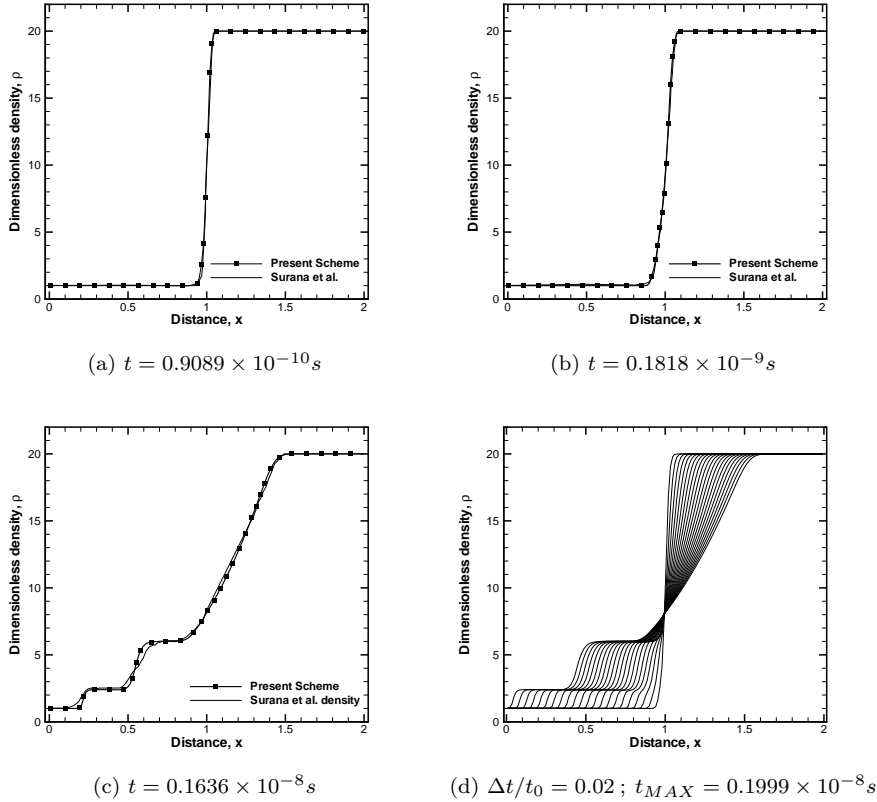


Figure 7: In (a), (b) and (c): comparison of density profiles u obtained by Surana *et al.* [1] and by DEM, respectively in the first, second and eighteenth time-step. (d) Evolution of velocity obtained with DEM.

6.3 Two-phases flow problem

In this case, the left and the right side of the shock tube are filled out with water and air at the same volume fraction equal to 0.5. The pressure is equal to 10^9 Pa on the left side and to 10^5 Pa on the right side. The discontinuity is initially located at $x=0.5$ m. The initial velocity is equal to zero for each phase. The profiles are shown at a time of 193.744 [μs]. The approximate solutions are computed with a 1000 points mesh. Also in this case, the results obtained using an Eulerian and a Viscous formulation are shown (Fig.(9)).

The same conclusions drawn in the previous section, can be used for these results, *i.e.* there are not differences between the two computations (Fig.(9)).

7 Conclusions

We have described a semi-discrete scheme for the resolution of interface problems when the effects of viscosity are taken into account. The DEM method, proposed by Abgrall and Saurel [7] has been used.

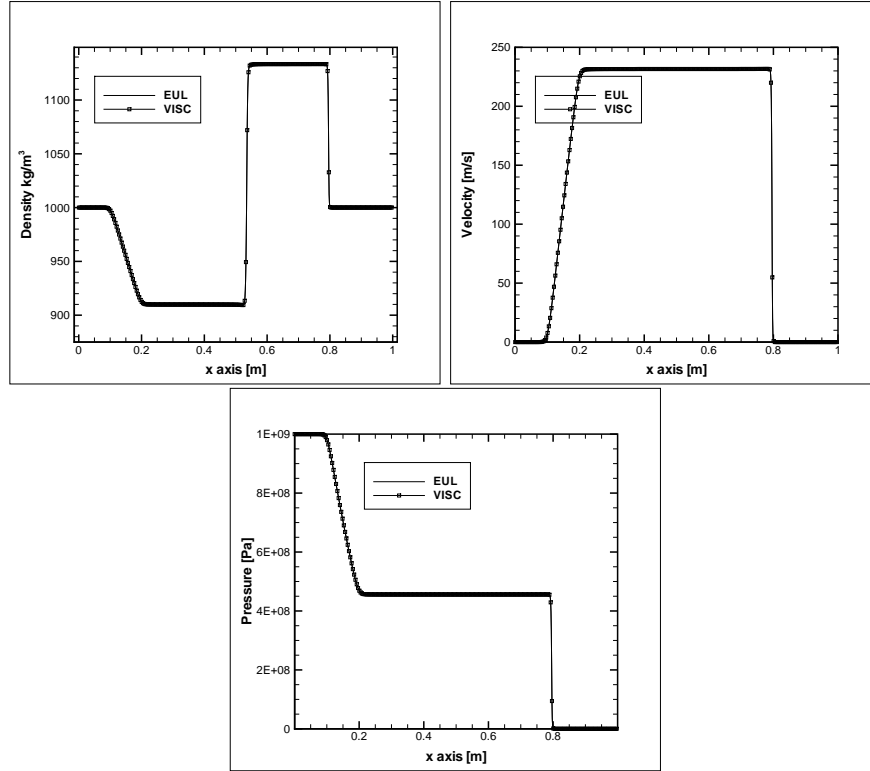


Figure 8: Single fluid test

The originality of this work is to analyze and to include, into the original scheme, the viscous flux of each phase, generated in the cell and through its boundary. The semi-discrete scheme for a seven equation model with viscous effects has been obtained for a first and a second order. A development of an asymptotic expansion of the scheme has been obtained in the limit of zero relaxation time of pressure and velocity. In particular, using the procedure proposed by Abgrall and Perrier [11], a semi-discrete scheme for the modelization of a reduced model of five equations including viscous effects in a configuration 1D, has been obtained.

The code has been validated with three test cases, that allowed showing some differences between the inviscid and viscous computations. In the first two tests, a non-physical viscosity of the fluids have been used in order to increase the effects of viscosity, showing a good behavior of the scheme for the discretization of viscous fluxes. Moreover, in the last validation test, our viscous solution has been compared with the numerical viscous solution, reported by Surana [1], showing a very good agreement between the results.

Successively, two others cases have been reproduced, showing that if the mesh is too coarse with respect to the shock thickness no significant differences can be observed between the viscous and non-viscous solutions.

This work is a fundamental step for the extension to the multi-dimension configuration, where the effect of viscosity is of primary importance to attain a good prediction of the numerical simulation.

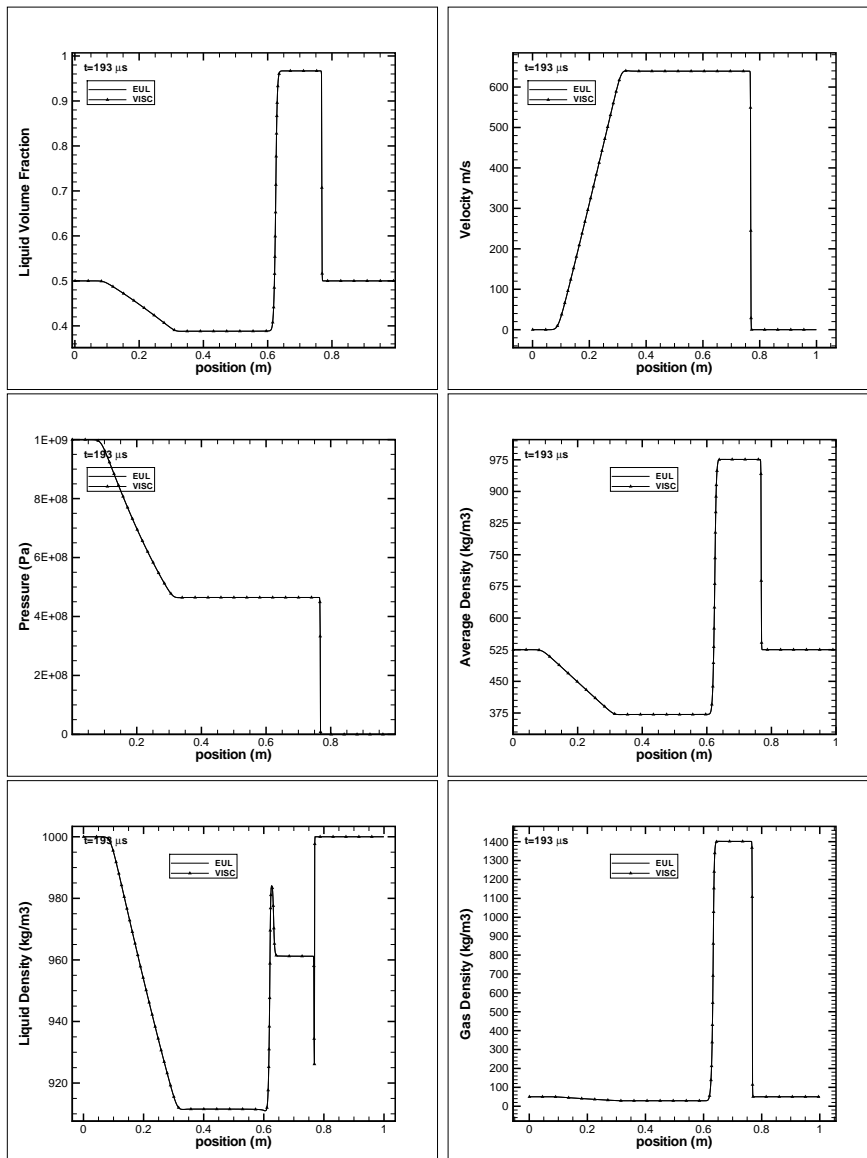


Figure 9: Two-phase flow problem

References

- [1] K.S. Surana, S. Allu, A.Romkes, and J.N. Redy. Evolution, propagation, reflection and interactions of 1d-normal shocks in air and fc70 using hpk finite element computational framework. *International Journal for Computational Methods in Engineering Science and Mechanics*, 10:370–392, 2009.
- [2] G. Allaire, S. Clerc, and S. Kokh. A five-equation model for the simulation of interfaces between compressible fluids. *Journal of Computational Physics*, 181:577–616, 2002.
- [3] A. Murrone and P. Villedieu. Numerical modeling of dispersed two-phase flows. *Aerospace Lab Journal*, 2:1–13, 2011.
- [4] Y. Sun and C. Beckermann. Diffuse interface modeling of two-phase based on averaging:mass and momentum equations. *Physica D*, 198:281–308, 2004.
- [5] R. Saurel and R. Abgrall. A multiphase godunov method for compressible multifluid and multiphase flows. *Journal of Computational Physics*, 150:425–467, 1999.
- [6] J. Massoni, R. Saurel, B. Nkonga, and R. Abgrall. Proposition de méthodes et modèles eulériens pour les problèmes à interfaces entre fluides compressibles en présence de transfert de chaleur: Some models and eulerian methods for interface problems between compressible fluids with heat transfer. *International Journal of Heat and Mass Transfert*, 45:1287–1307, 2002.
- [7] R. Abgrall and R. Saurel. Discrete equations for physical and numerical compressible multiphase mixtures. *Journal of Computational Physics*, 186:361–396, 2003.
- [8] R. A. Berry, R. Saurel, and O. LeMetayer. A multiphase model with internal degrees of freedom:application to shock-bubble interaction. *Journal of Fluid Mechanics*, 496:283–321, 2003.
- [9] A. Murrone and H. Guillard. A five equation reduced model for compressible two-phase flow problems. *Journal of Computational Physics*, 202:664–698, 2004.
- [10] G.Perigaud and R. Saurel. A compressible flow model with capillary effects. *Journal of Computational Physics*, 209:139–178, 2005.
- [11] R. Abgrall and V. Perrier. Asymptotic expansion of multiscale numerical scheme for compressible multiscale flow. *Society for Industrial and Applied Mathematics*, 5:84–115, 2006.
- [12] D.A. Drew and S.L. Passman. *Theory of Multicomponent Fluids*, volume 135. Applied Mathematical Sciences, Springer, New York, 1998.
- [13] C. Hirsch. *Numerical Computational of Internal and External Flows. Volume 2: Computational Methods fo Inviscid and Viscous Flows*. John Wiley, Usa, 1988.

- [14] R. Saurel, S. Gavrilyuk, and F. Renaud. A multiphase model with internal degrees of freedom: application to shock-bubble interaction. *Journal of Fluid Mechanics*, 496:283–321, 2003.
- [15] H.W.Liepmann and A.Roshko. *Elements of gasdynamics*. John Wiley, Usa, 1957.



**RESEARCH CENTRE
BORDEAUX – SUD-OUEST**

351, Cours de la Libération
Bâtiment A 29
33405 Talence Cedex

Publisher
Inria
Domaine de Voluceau - Rocquencourt
BP 105 - 78153 Le Chesnay Cedex
inria.fr

ISSN 0249-6399